Content-sensitive superpixel generation with boundary adjustment.

ZHANG, D., XIE, G., REN, J., ZHANG, Z., BAO, W. and XU, X.

2020

applied sciences

Article

Content-Sensitive Superpixel Generation with Boundary Adjustment

Dong Zhang [1], Gang Xie [1,2,*], Jinchang Ren [1,3,4,*], Zhe Zhang [1], Wenliang Bao [5] and Xinying Xu [1]

[1] College of Electrical and Power Engineering, Taiyuan University of Technology, Taiyuan 030024, China; zhangdong0285@link.tyut.edu.cn (D.Z.); zhangzhe@tyut.edu.cn (Z.Z.); xuxinying@tyut.edu.cn (X.X.)
[2] Shanxi Key Laboratory of Advanced Control and Intelligent Information System, Taiyuan 030024, China
[3] Department of Electronic and Electrical Engineering, University of Strathclyde, Glasgow G11XW, UK
[4] College of Electronics and Information, Xi'an Polytechnic University, Xi'an 710048, China
[5] Taiyuan Research Institute, China Coal Technology and Engineering Group, Taiyuan 030006, China; bao_wl@126.com
* Correspondence: xiegang@tyut.edu.cn (G.X.); jinchang.ren@strath.ac.uk (J.R.)

Received: 23 March 2020; Accepted: 27 April 2020; Published: 30 April 2020

Abstract: Superpixel segmentation has become a crucial tool in many image processing and computer vision applications. In this paper, a novel content-sensitive superpixel generation algorithm with boundary adjustment is proposed. First, the image local entropy was used to measure the amount of information in the image, and the amount of information was evenly distributed to each seed. It placed more seeds to achieve the lower under-segmentation in content-dense regions, and placed the fewer seeds to increase computational efficiency in content-sparse regions. Second, the Prim algorithm was adopted to generate uniform superpixels efficiently. Third, a boundary adjustment strategy with the adaptive distance further optimized the superpixels to improve the performance of the superpixel. Experimental results on the Berkeley Segmentation Database show that our method outperforms competing methods under evaluation metrics.

Keywords: content-sensitive; superpixel; boundary adjustment

1. Introduction

Dividing an image into several simple connected regions with perceptual meanings is called superpixels. Superpixels can represent images more concisely and efficiently than pixels, which can significantly reduce the complexity of subsequent image processing. After the concept of superpixels was proposed by Ren and Malik [1] in 2003, the simplified image expression became a key step in many computer vision tasks, such as segmentation [2–6], saliency detection [7–9], object recognition [10,11], modelling [12,13], 3D reconstruction [14], and other vision tasks [15–17]. For these applications, the high-quality superpixels are desired to meet the following properties:

1. Each superpixel is a simple single connected area with the regular shape.
2. Superpixels should adhere well to the image boundaries and pixels inside the superpixels should have homologous characteristics.
3. The density of superpixels should be adaptive to local image content.
4. The superpixels algorithms should be fast to compute and memory efficient.

The superpixel segmentation algorithms can be roughly divided into two categories: Graph-based methods and clustering-based methods. Graph-based methods treat each pixel as a vertex in the graph. The similarity between adjacent pixels is considered as the weight of the edge. The normalized cut

(N-cut) algorithm [18] recursively partitions the pixel graph using contour and texture information in the image. Felzenszwalb and Huttenlocher [19] proposed a superpixel generation method based on the minimum spanning tree (FH). Moore et al. [20] generated superpixels (SL) by searching the minimum path from the horizontal and vertical directions. Veksler et al. [21] generated superpixels (Graph Cut) by half-overlapping square patches of the same size covered on the image. Liu et al. [22] presented a graph-based approach (ERS), which combines the entropy rate of a random walk with and a balancing function for superpixel segmentation. SEEDS [23] generates superpixels by iteratively modifying the initial approximate boundaries of superpixels according to the energy function.

The clustering-based methods define a distance measure to evaluate the similarity between pixels and generate superpixels by iteratively assigning pixels to the most similar seeds until some convergence criteria are reached. TurboPixels [24] is a geometric flow method (TP), which regularly places the seeds on images and grows the superpixels by level-set. This method can make the size of superpixels uniform, but it consumes more time than other superpixel methods.

Zeng et al. [25] proposed structure-sensitive superpixels (SSS) according to the geodesic distance computed from geometric flows. SSS can effectively describe the nonhomogenous features in images by the superpixel size. However, the computational cost of SSS is even higher than that of TP.

Achanta et al. [26] proposed an algorithm, simple linear iterative clustering (SLIC), to generate superpixels. SLIC uniformly places the initial cluster centers on the geometric center of the regular grids. By limiting the search range of the k-means algorithm, the computational complexity of the SLIC is greatly reduced. To further improve the performance of SLIC, Achanta and Susstrunk [27] proposed simple non-iterative clustering (SNIC) to compute superpixels with one iteration.

Liu et al. [28] proposed manifold SLIC (MSLIC), which expands SLIC to generate content-sensitive superpixels. MSLIC maps a five-dimensional image space to a two-dimensional manifold for computing restricted centroidal Voronoi tessellation under the Euclidean metric. As an improvement of MSLIC, the authors proposed intrinsic manifold SLIC [29] (IMSLIC) to compute a centroidal Voronoi tessellation under the geodesic distance instead of Euclidean distance on the image manifold.

Shen et al. [30] presented the lazy random walk (LRW) method to evaluate the probabilities between a seed and its neighbor pixels. The authors [31] also proposed a real-time superpixel segmentation method (DBSCAN) to apply density-based spatial clustering. Small initial superpixels are further merged with adjacent superpixels to ensure connected superpixels.

Li and Chen [32] proposed the linear spectral clustering (LSC) to generate superpixels based on simple k-means clustering. The algorithm maps a five-dimensional color space into a ten-dimensional space, resulting in superpixels with high boundary adherence.

All the above clustering-based methods usually consist of two steps: (1) Regular initialization of seeds to generate superpixel, and (2) update seeds to the center of mass. The results of this algorithm depend on the initial position of seeds, and the seed regular initialization ignores the content sensitivity. To address this issue, we propose a novel superpixel segmentation algorithm, which adopts the image local entropy and the boundary adjustment strategy to generate superpixels. In summary, the contribution of this paper includes the following three respects:

1. The seeds initialized by most cluster-based superpixel algorithms are spatially uniform. Our method introduces image entropy at seeds sampling, which aims at generating content-sensitive superpixels to improve the accuracy of superpixel segmentation. The image local entropy can well measure the content sensitivity of the image and can initialize the seeds at a lower computational cost.
2. We used boundary adjustment to optimize superpixels. Adaptive boundary adjustment can generate regular superpixels in sparse content areas and superpixels with good boundary adherence in dense content areas, and the boundary adjustment can quickly converge.
3. The proposed algorithm was evaluated on the Berkeley Segmentation Database (BSDS 500) [33]. Compared with other five methods, the algorithm achieved better segmentation accuracy while ensuring superpixel compactness.

The rest of the paper is organized as follows. The Section 2 introduces our method and analyzes the parameters in detail. The experimental results, compared with the five representative methods, are shown in Section 3. Experimental results are discussed in Section 4. In Section 5, we show the foreground segmentation performance of the superpixel algorithm proposed in contour closure. Finally, a brief summary is made in Section 6.

2. Materials and Methods

This paper develops a novel method for generating content-sensitive superpixels, which improves the performance of segmentation algorithms. The proposed algorithm has three phases. The first phase is seed sampling for adaptive image content. The second phase is clustering superpixels based on the minimum spanning tree algorithm. The third phase is the boundary adjustment phase, in which the distance measure of adaptive weights is adopted to improve the segmentation quality.

2.1. Seed Sampling Strategy

Any natural image contains a lot of uneven image information. The change in the local color intensity of the image reflects the change in the amount of local information. Therefore, it is but natural to place more seeds in content-dense regions of the image and to place fewer seeds in content-sparse regions of the image. However, the uniformity of seeds is also strongly important for the compactness of superpixels. Then, the proposed seeds distribution strategy based on image local entropy achieved a balance between the content sensitivity and uniformity of seeds. The heterogeneity of each pixel was captured using Normalized Shannon Entropy. The entropy operator calculates the entropy of the pixel value in the neighbor center. Let the pixel gray values in the center and the N neighbor pixels be a_0, a_1, a_2, ... , a_N, respectively. The entropy operator is given in Table 1.

Table 1. Entropy operator.

a_1	a_2	a_3	$H=-\sum_{i=0}^{N} P_i \log P_i / \log(N+1)$
a_4	a_0	a_5	
a_6	a_7	a_8	$P_i = a_i / \sum_{j=0}^{N} a_j$

The entropy H was normalized so that $H \in [0,1]$. For color images in the CIELAB color space $\mathbf{c} = \begin{bmatrix} l & a & b \end{bmatrix}^T$, the image local entropy is defined as

$$H = q_l H_l + q_a H_a + q_b H_b \tag{1}$$

where

$$\begin{cases} q_l = l/(l+a+b) \\ q_a = a/(l+a+b) \\ q_b = b/(l+a+b) \end{cases} \tag{2}$$

Both brightness information and tone information were used to measure the local entropy carried by natural color images. Therefore, when the brightness or the color tone of the region changed greatly, the entropy value of the color image was small. The part of the image should contain more information when the color intensity of the part of the image changes drastically, and vice versa. For neighborhood center i, the local information of each pixel $I(i)$ is defined as

$$I(i) = \omega \log(1 + (1 - H) \times 10^{\gamma}) \tag{3}$$

where ω and γ are scaling parameters.

We outline seed sampling strategy in Algorithm 1. Different from the placement method of simple regular grids seeds [26] and two-level quad-tree split-up seeds [25], the proposed approach considered the local information of the image in the process of placing seeds. In order to make each superpixel contain an approximate amount of image information, the information interval was $s = \sum_{i=1}^{n} I(i)/k$, where n is the number of pixels in the image and k is the desired number of superpixels. The images were scanned from left to right and from top to bottom, and the pixels were added that were four- or eight-connected to the currently growing region. When the scanned pixels reached the information interval, the seed was placed. For an initial superpixel S_i, its position center $\mathbf{x}_i = \begin{bmatrix} x_i & y_i \end{bmatrix}^T$ is

$$x_i = \frac{\int_{x \in S_i} x dx}{\int_{x \in S_i} 1 dx}, \; \mathrm{y}_i = \frac{\int_{y \in S_i} y dy}{\int_{y \in S_i} 1 dy}, \tag{4}$$

Algorithm 1. Seed sampling strategy

```
Input: An image $I$ of $n$ pixels, the desired number of superpixels $k$, and the parameters $\gamma$ and $\omega$
Output: $k$ seeds of the image $I$
Calculate the local information of each pixel $I(i)$
Calculate information interval $s = \sum_{i=1}^{n} I(i)/k$ of image $I$
for each pixel $p_i$ do
  if the pixel is not scanned then
    Store $p_i$ as region $S_i$
    for each connected neighbor $p_j$ of $S_i$ do
      if the pixel is not scanned then
        $I(i) \leftarrow I(i) + I(j)$
        $x_i \leftarrow x_i + x_j$
        $y_i \leftarrow y_i + y_j$
        Add $p_j$ to region $S_i$
        if $I(i) > s$ then
          break
        end if
      end if
    end for
  end if
  Place seed using Equation (4)
end for
```

2.2. Minimum Spanning Tree Clustering

An image can be converted to an undirected graph $\mathcal{G} = (\mathcal{V}, \mathcal{E})$, whose pixels in the image $v \in \mathcal{V}$ are the vertices and the value of each edge $e_{ij} = \left(v_i, v_j\right)$ evaluates the similarity between the two vertices $e \in \mathcal{E} \subseteq \mathcal{V} \times \mathcal{V}$. Let k be the number of superpixels to be divided, the superpixel segmentation task is broken up the undirected graph $\mathcal{G}$ into k disjoint subgraphs $\mathcal{G}' = (\mathcal{V}', \mathcal{E}')$, where $\mathcal{V}' \subseteq \mathcal{V}$ and $\mathcal{E}' \subseteq \mathcal{E}$.

The proposed algorithm is a kind of bottom-up pixel aggregation method, which grows regions based on the Prim method [34]. The Prim algorithm is a greedy algorithm that finds the minimum spanning tree for a weighted undirected graph. Suppose a graph has n vertices, and the goal is to aggregate the vertices into a forest with k trees. Starting from the initial seeds, the algorithm adds the least cost connection from the tree to the vertex in each step. Similar to SLIC [26], a distance measure was adopted in five-dimensional space. In the spatial space $\mathbf{x} = \begin{bmatrix} x & y \end{bmatrix}^T$ and CIELAB color space $\mathbf{c} = \begin{bmatrix} l & a & b \end{bmatrix}^T$, the distance of two vertices v_1 and v_2 is defined as

$$D(v_1, v_2) = \sqrt{\lambda^2 \frac{\|\mathbf{x}_1 - \mathbf{x}_2\|_2^2}{N_x^2} + \|\mathbf{c}_1 - \mathbf{c}_2\|_2^2} \tag{5}$$

where N_x is a normalization parameter. For an image of n pixels, the value of N_x is set to be $\sqrt{n/k}$. The value of λ is set by the user. λ weighs the relative importance of the color distance term and spatial distance term. The larger the λ value is, the more regular the generated superpixels are. The smaller the λ value is, the boundary adherence better the generated superpixels are.

The Prim algorithm only considers the distance between two vertices on the tree border during the aggregation process. This metric is extremely sensitive to noise. The average attributes of the tree are used to calculate the distance, which not only simplifies the calculation of the shortest path distance in the neighbor, but also improves the robustness of the Prim algorithm. After running the Prim algorithm, k trees representing k superpixels are generated. For a superpixel S_i, its average attribute $C_i = \begin{bmatrix} \mathbf{x}_i & \mathbf{c}_i \end{bmatrix}$ is given by

$$C_i = \frac{\int_{v \in S_i} v dv}{\int_{v \in S_i} 1 dv} \tag{6}$$

The average attribute replaces the seed to calculate the distance. Figure 1 illustrates this aggregation process of superpixels. The process of minimum spanning tree clustering is summarized in Algorithm 2.

Algorithm 2. Minimum Spanning Tree Clustering

```
**Input:** An image $I$ of $n$ pixels, $k$ initial locations $\mathbf{x}_i$ generated in Algorithm 1 and the weight parameter $\lambda$
**Output:** Initial Superpixel label map $L$
Initialize $L[:] \leftarrow -1$
Initialize $C_i = \begin{bmatrix} \mathbf{x}_i & \mathbf{c}_i \end{bmatrix}$ by extracting the features of the initial locations $\mathbf{x}_i$
**for** each centroid $C_i$ **do**
  Vertex $v \leftarrow \begin{Bmatrix} C_i & k & 0 \end{Bmatrix}$
  Push $v$ on priority queue $Q$
**end for**
**while** $Q \neq \varnothing$ **do**
  remove $v_i$ from the priority queue $Q$
  $L[v_i] = k_i$
  Update the centroid $C_i$ using Equation (6)
  **for** Each connected neighbor $v_j$ of $v_i$ **do**
    Calculated distance of $v_j$ and $v_i$ using Equation (5)
    Create the Vertex $v_j \leftarrow \begin{Bmatrix} C_j & k_i & d_{ij} \end{Bmatrix}$
    **if** $L[:] \leftarrow -1$ **then**
      Push $v_j$ on $Q$
    **end if**
  **end for**
**end while**
```

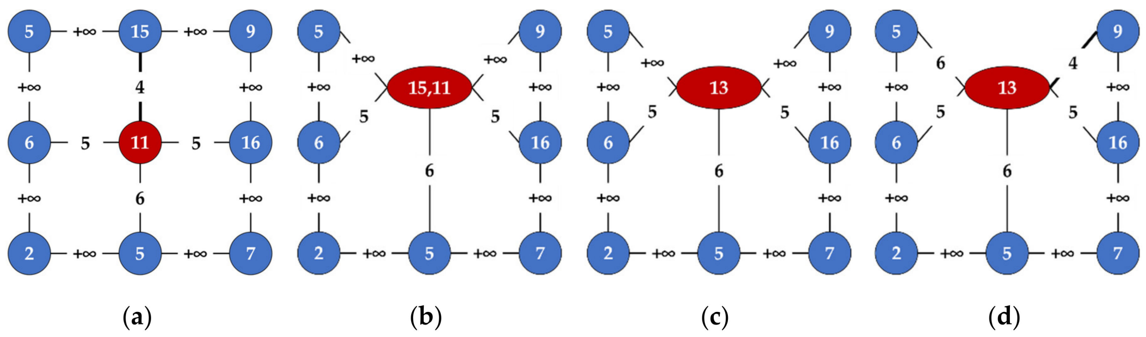

Figure 1. Illustration of the aggregation process of superpixels. The vertices represent pixels and the edges represent similarities. (**a**)The vertex 15 is the nearest neighbor of the tree (red vertex 11), (**b**) the tree aggregates the nearest neighbor, (**c**) update the average attribute of the tree, (**d**) expand the search scope of the tree and find the next nearest neighbor(vertex 9).

2.3. Boundary Adjustment

The preliminary segmentation results were formed at one time and further optimization was required. In Figure 2, the shape of the superpixel was not regular enough, especially in the content-sparse region. There were several under-segmentation errors in the area pointed by the red arrow in the image. It can be seen that boundary adjustment significantly improved the compactness and boundary adherence of superpixels.

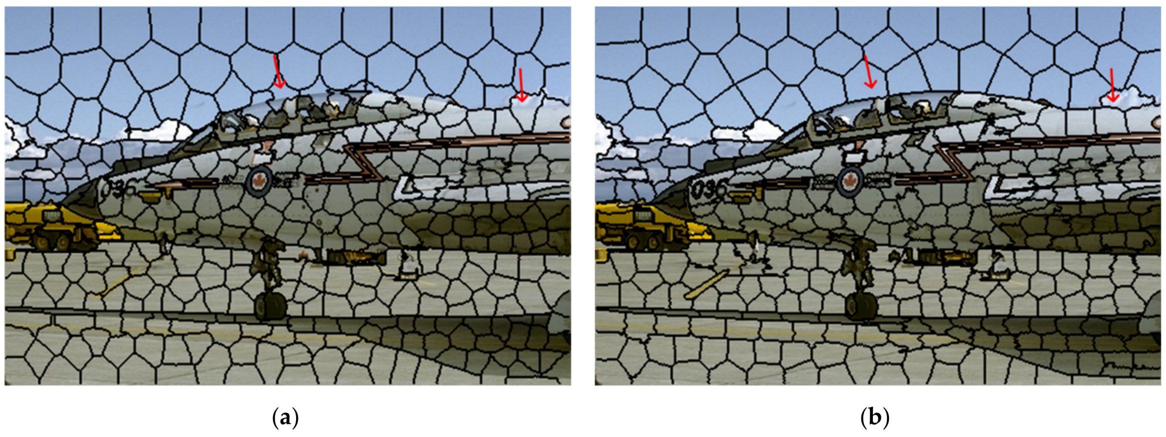

Figure 2. Image segmentation results with 400 superpixels. (**a**) Superpixel segmentation results after minimum spanning tree clustering, (**b**) superpixel segmentation results after boundary adjustment.

The boundary pixels of the initial superpixels were allocated to obtain better compactness and boundary adherence. Among pixels connected to S_i, the pixels that do not belong to S_i are boundary pixels. For each boundary pixel, calculate the distance between the boundary pixel and the adjacent superpixel, and assign the boundary pixel to the superpixel which is nearest to it. Boundary adjustment is an iterative process. The iteration is terminated when the set number of iterations is reached.

In the distance Equation (5), the color distance term affects the adherence of superpixels boundary, and spatial distance term affects the compactness of superpixels. To enhance the content sensitivity of superpixels, we define the new distance measurement as follows:

$$D'(v_1, v_2) = \sqrt{\lambda^2 \frac{\|\mathbf{x}_1 - \mathbf{x}_2\|_2^2}{N_x^2} + \|\mathbf{c}_1 - \mathbf{c}_2\|_2^2 \cdot I(i)} \tag{7}$$

When the value $I(i)$ is higher, the color distance is more considered. When the value $I(i)$ is lower, the spatial distances should be more considered.

Boundary adjustment does not guarantee the superpixel connectivity. In the procedure, a superpixel may be split into several unconnected sub-superpixels. Connectivity is taken into account of the procedure of boundary adjustment and additional steps are not required. For too small sub-superpixels, they will merge with the nearest superpixel. The pseudo code of boundary adjustment is presented Algorithm 3.

Algorithm 3. Boundary adjustment

```
Input: Initial Superpixel label map $L$ and the maximum number of iterations $Maxiter$
Output: Optimized Superpixel label map $L$
While iter < $Maxiter$ do
  for each superpixel $S_i$ do
    for each boundary vertex $v_i$ do
      for Each connected neighbor $v_j$ of $v_i$ that are not in $S_i$ do
        Get the superpixel $S_j$ which $v_j$ belongs to
        Compute $D'(v_j, C_j)$ and $D'(v_j, C_i)$ using Equation (7)
        if $D'(v_j, C_i) < D(v_j, C_j)$ then
          $L[v_j] = k_i$
          Update $C_i$ and $C_j$ using Equation (6)
          Update the boundary vertices
        end if
      end for
    end for
  end for
end while
```

For an image with n pixels, it is obvious that the complexity of the image local entropy and the seed sampling strategy are O(n). In the minimum spanning tree clustering phase, the number of pixels in the priority queue is much smaller than n. Thereby, the impact of priority queues on computational complexity is not very obvious. In the boundary adjustment stage, the computational cost in each iteration is O(n_B), in which n_B is the number of boundary pixels. In practice, $n_B \ll n$. In the comprehensive analysis, the proposed algorithm is of linear complexity O(n).

2.4. Datasets and Performance Metrics

We adopted the commonly used evaluation metrics in the literature of superpixel segmentation to evaluate superpixel segmentation algorithms, including boundary recall (BR), achievable segmentation accuracy (ASA), and under-segmentation error (USE). The BSDS 500 [33] consisted of 500 images with manually labeled ground truth segmentations. In the following experiments, the methods were evaluated using the average performance metrics of five hundred images in the BSDS 500 [33].

Boundary recall (BR) measures the fraction of the ground truth boundary identifications. A high BR represents the better boundary adherence with respect to the ground truth boundaries. Given a ground truth boundary sets $B(g)$ and the superpixel boundary sets $B(s)$, then BR is defined as:

$$BR = \frac{\mathrm{TP}(B(g), B(s))}{\mathrm{TP}(B(g), B(s)) + \mathrm{FN}(B(g), B(s))} \tag{8}$$

Let FN ($B(g)$, $B(s)$) and TP ($B(g)$, $B(s)$) be the number of false negative and true positive boundary pixels. $B(s)$ is matched to $B(g)$ within a local neighbor with size $(2r + 1) \times (2r + 1)$. In practice, r is set to 1.

Achievable segmentation accuracy (ASA) computes the upper bound of accuracy using superpixels as preprocessing step. Denote a ground truth segmentation of an image as $\{G_i|i = 1, 2, \cdots, M\}$ and a superpixel segmentation as $\{S_l|l = 1, 2, \cdots, K\}$. The ASA metric is defined as follows:

$$\text{ASA} = \frac{\sum\limits_{S_l} \max_{G_i}\{|S_l \cap G_i|\}}{\sum\limits_{G_i} |G_i|} \tag{9}$$

where |.| is the number of a superpixel in pixel. In general, a high ASA demonstrates that superpixels match the objects well in the image.

Under-segmentation error (USE) measures the "leakage" of superpixels from the ground truth boundaries, which is calculated by:

$$\text{USE} = \frac{1}{n} \sum_{S_l} \left| S_l - \text{argmax}_{G_i} |S_l \cap G_i| \right| \tag{10}$$

where n is the total number of pixels in the image. Each superpixel was assigned to the ground truth segments with the largest overlap, and only the "leakage" with respect to other ground truth segments was considered. Therefore, USE implicitly also measures boundary adherence. A lower USE refers to that superpixels overlap with a ground truth segmentation more accurately.

2.5. Parameter Selection

In the proposed method, γ, ω, λ, and *Maxiter* should be set in advance. The following experiments use various values to investigate the parameters.

The measure of image information contains two parameters, γ and ω. γ is used to adjust the uniformity and content sensitivity of the seeds. As shown in Figure 3, with the increasing values of γ, the value of performance metrics changes significantly because small γ values imply the seeds are too sensitive to the image content and concentrated in complex areas while ignoring other areas. When γ becomes too large, the distribution of seeds tends to regular grid seeds, and the content sensitivity is ignored. ω is used to adjust the proportion of the color term in Equation (7). In practice, we truly use their product, $p = \omega \cdot \gamma$. Approximately, the values of $I(i)$ fall in the interval [0, p]. As shown in Figure 4, when p increases, more detailed information is considered and the resulting superpixels are more irregular.

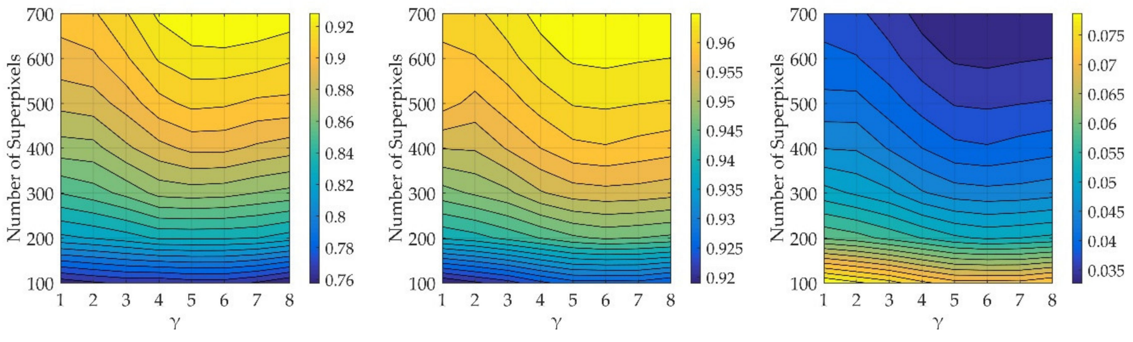

(**a**) BR (**b**) ASA (**c**) USE

Figure 3. The performance metrics of our approach with different γ values.

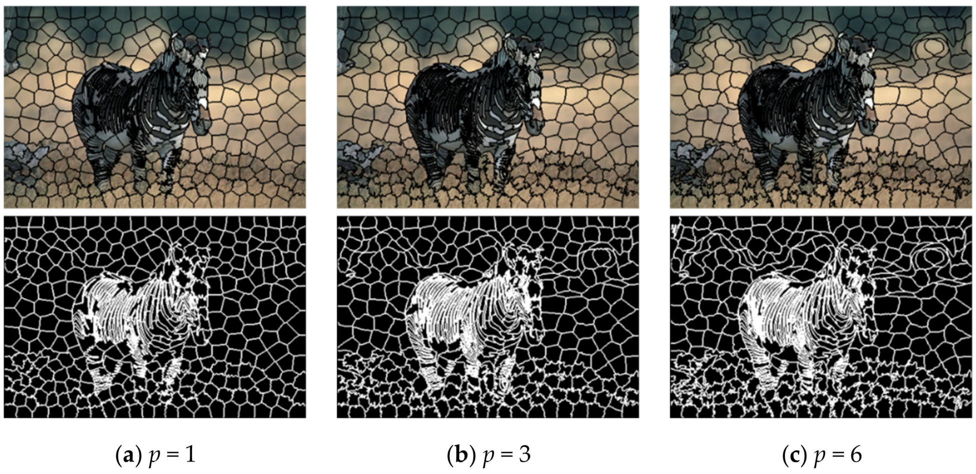

Figure 4. Superpixel segmentation results with different p values.

λ represents the weight parameters of the distance measure in the stage of minimum spanning tree clustering. Particularly, when $\lambda \rightarrow \infty$, the generated superpixels are regularly grid only related to the position of the initial seeds. When $\lambda = 0$, the pixels with similar colors are clustered to generate irregular superpixels. The trend is shown in Figure 5. Figure 6 shows the average values of BR, ASA, and USE on the BSDS 500 for different λ values when K = 400. Overall, the performance metrics becomes worse as the value of λ increases.

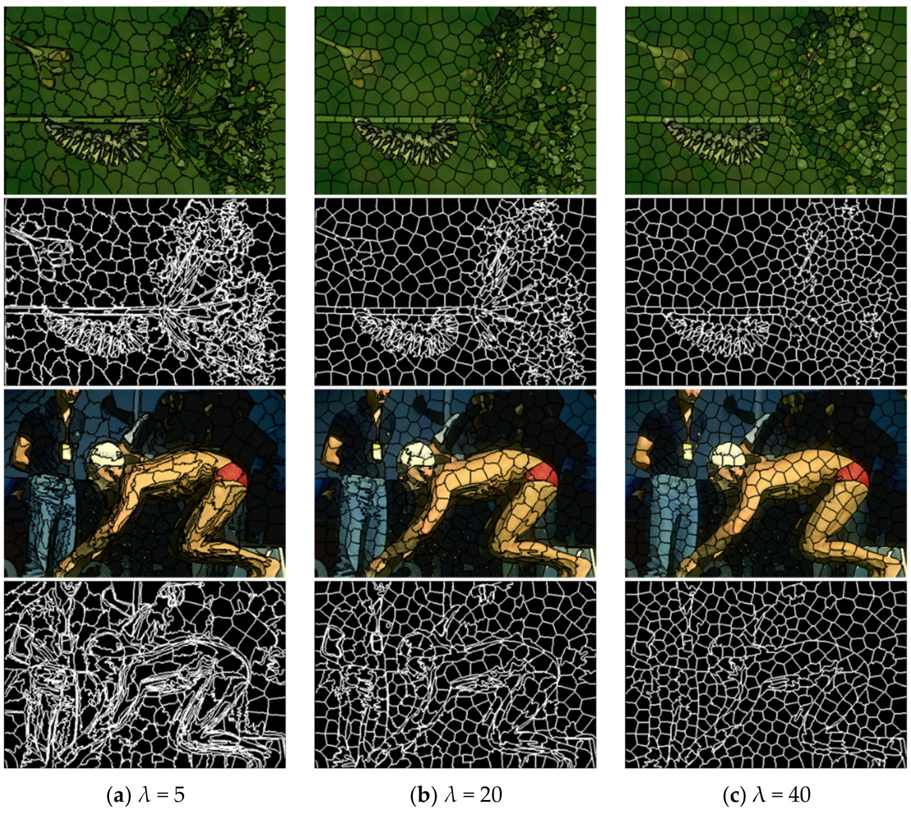

Figure 5. Superpixel segmentation results with different λ values.

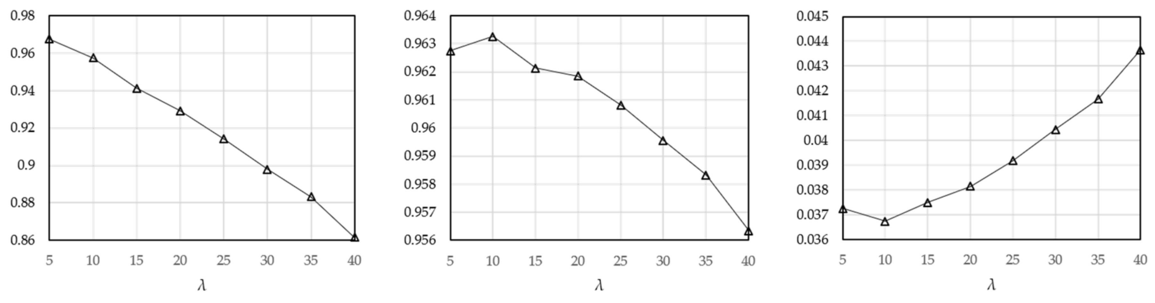

(**a**) BR (**b**) ASA (**c**) USE

Figure 6. The performance metrics of our approach with different λ values at k = 400.

The number of iterations *Maxiter* can balance time cost and performance. The metrics with *Maxiter* are shown in Figure 7. It is easy to find that our algorithm can quickly converge after two iterations. More iterations will only increase time consumption. Also shown in Figure 2, the superpixels became more compact after iterations.

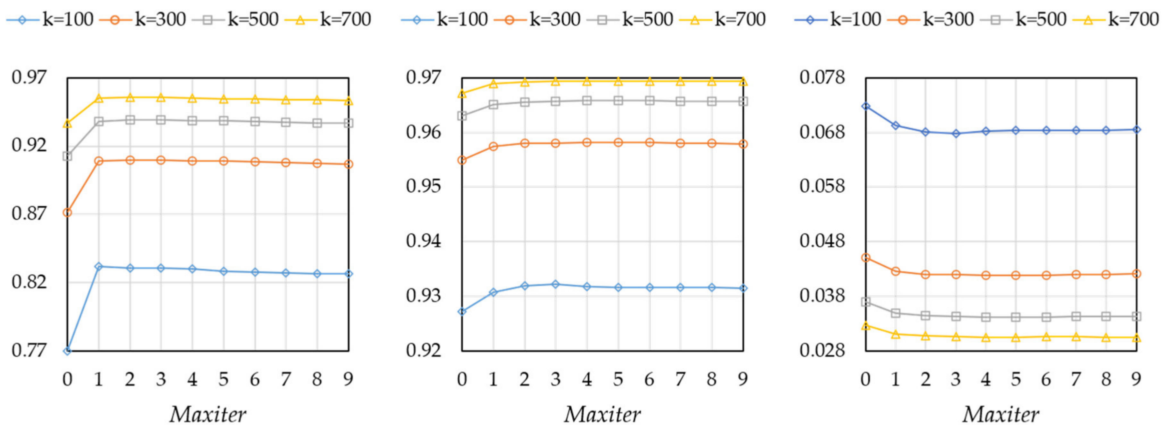

(**a**) BR (**b**) ASA (**c**) USE

Figure 7. The performance metrics of our approach for different *Maxiter* values.

From the discussion above, we select γ = 6 and *Maxiter* = 3, where achieve the best performance. Considering the accuracy and compactness of superpixels, we empirically select λ = 20 and p = 3.

3. Results

The proposed algorithm was implemented in C++ and tested on a PC with an Intel i5-8300H CPU (2.30 GHz) and 8GB RAM. The performance of the proposed algorithm was compared with the five representative superpixel generation algorithms, including SLIC [26], SNIC [27], ERS [22], LSC [32], and FH [19]. We used the implementations available online for all other methods. To ensure segmentation performance, all algorithms were run on the recommended parameters. The comparison experiment results on BSDS 500 [33] are shown in Figure 8. As a preprocessing step for image processing, the time cost was also an important indicator. In Figure 8d, we also compared the efficiency in the average running time per image. Table 2 presents the mean and standard deviation performance metrics at k = 400. A visual comparison is displayed in Figure 9.

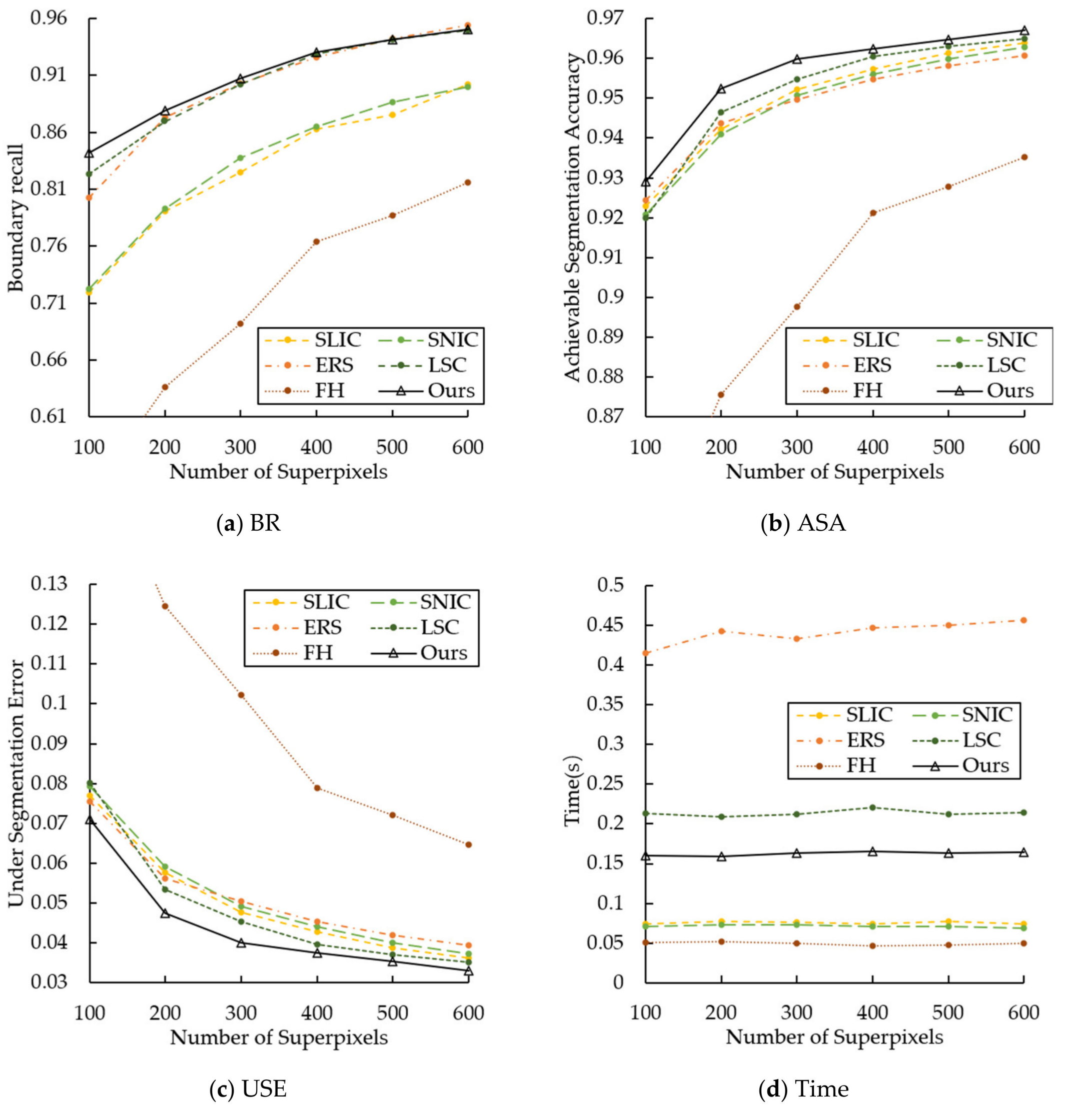

Figure 8. Quantitative evaluation of different superpixel segmentation algorithms.

Table 2. Performance metrics of different superpixel segmentation algorithms at k = 400.

	BR	ASA	USE	Computational Complexity	Average Time Per Image
SLIC [26]	0.863 ± 0.064	0.957 ± 0.021	0.042 ± 0.021	O(n)	0.076 s
SNIC [27]	0.865 ± 0.062	0.955 ± 0.022	0.044 ± 0.022	O(n)	0.070 s
ERS [22]	0.925 ± 0.040	0.954 ± 0.024	0.045 ± 0.024	O(n^2 log n)	0.442 s
LSC [32]	0.928 ± 0.040	0.960 ± 0.020	0.039 ± 0.020	O(n)	0.220 s
FH [19]	0.763 ± 0.102	0.921 ± 0.042	0.078 ± 0.042	O(n log n)	**0.051 s**
Ours	**0.931 ± 0.046**	**0.962 ± 0.020**	**0.038 ± 0.020**	O(n)	0.159s

Bold indicates the best value of the corresponding metric.

A good initialization is essential for superpixel algorithms. In Section 2.1, we propose a seed sampling strategy different from regular grid initialization, which introduces image entropy into seed sampling strategy to optimize the content sensitivity of the seed. Furthermore, the content initialization compares with regular initialization in the proposed method on the entire BSDS 500 dataset. The results under the three metrics (i.e., USE, BR, and ASA) are reported in Figure 10, which shows that our sampling strategy is better than regular grid initialization.

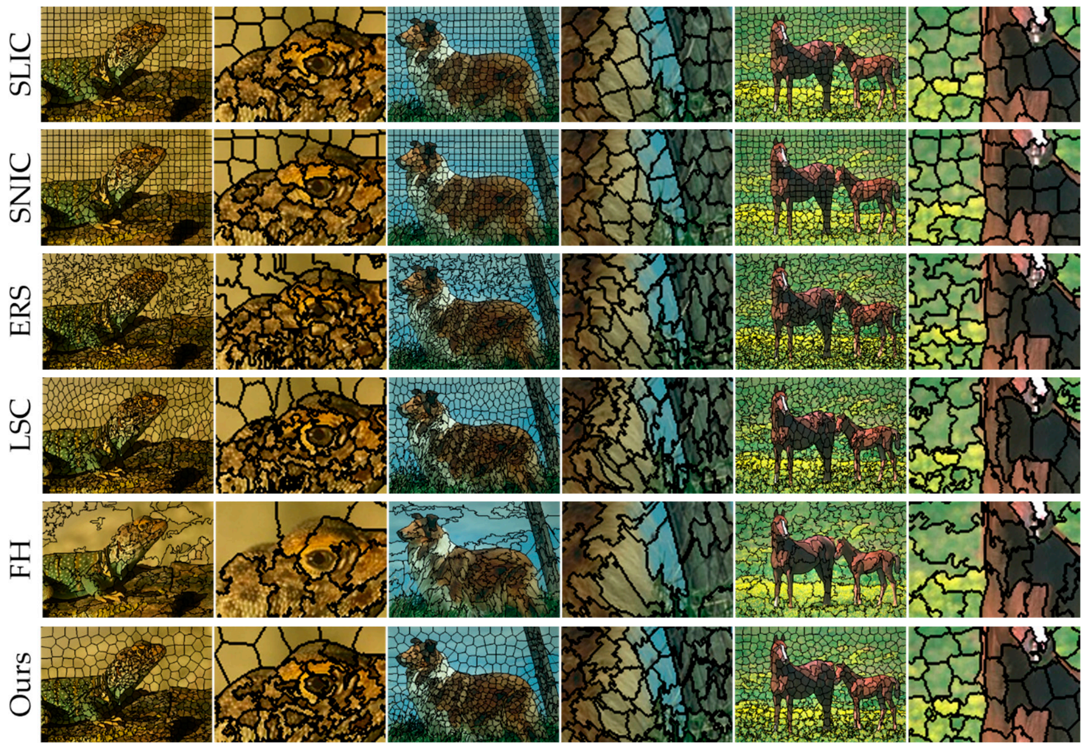

Figure 9. Visual comparison of superpixel segmentation results using different algorithms.

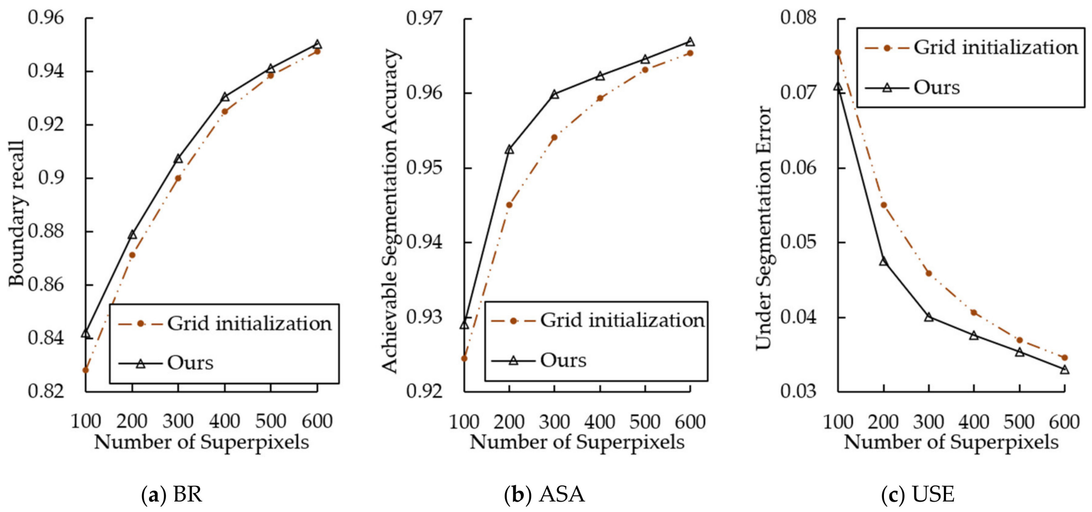

Figure 10. The metrics value comparison of our seed sampling strategy and grid initializations.

4. Discussion

Referring to the plots in Figure 8, our method is superior to the other five methods in terms of ASA and USE. The LSC, ERS, and our method exhibit high performance on BR. However, our approach is more competitive at a lower set number of superpixels. As a preprocessing step, generating a lower number of high-quality superpixels is more helpful for subsequent tasks. From Figure 8 and Table 2, it can be seen that the proposed method is comparable to the other five representative methods in terms of boundary adherence.

Figure 9 shows the visual results of superpixel segmentation using these algorithms. Enlarge the local segmentation results for detailed inspection. Visually, our method had the most satisfactory segmentation results for different types of images. SLIC, SNIC, and our method showed the best compactness. However, compared with the proposed algorithm, SLIC and SNIC had weaker boundary adherence. The boundary adherence of ERS was very competitive, but the compactness of ERS was not satisfactory. LSC produced competitive results and performed well in compactness and boundary adherence. LSC introduces global information to generate superpixels, which makes it requires 20 iterations. From Figure 8d, LSC took longer to run than our method. In addition, our method can exceed the performance of LSC by adjusting parameters, but it sacrifices compactness. Superpixels generated by FH and the proposed method exhibited content sensitivity. Due to the lack of compactness constraints, the superpixels produced by FH were extremely irregular and under-segmented in content-rich areas. The results show that the algorithm achieves good boundary adherence while ensuring good compactness.

5. Application to Image Contour Closure

We investigated the effect of segmentation using different superpixels in image contour closure applications. Superpixel is a preprocessing step to reduce the complexity of subsequent image tasks. Levinshtein et al. [6] proposed an energy framework to search for a subset of superpixels to obtain the contour of strong edge support in an image. The energy framework proposed by Levinshtein et al. was used to compare six superpixel algorithms. The energy framework was applied to the Weizmann Segmentation Evaluation Database (WSED) [35], which consists of 100 images with human-annotated ground truth segmentations for each image. The average F-measure, precision, and recall are summarized in Table 3. Figure 11 also shows the qualitative results of the four examples. Both quantitative and qualitative results show that the proposed method has good foreground segmentation performance.

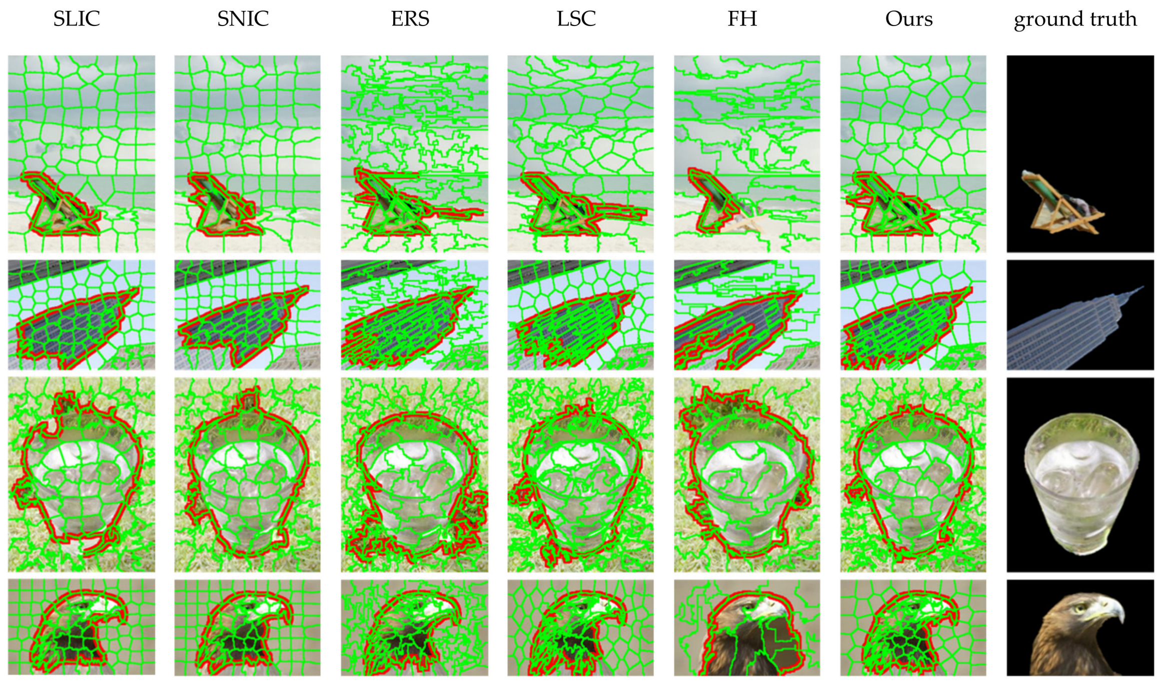

Figure 11. Visual comparison of contour closure results on four examples in Weizmann Segmentation Evaluation Database (WSED). The superpixel boundaries are shown in green, and the closure contours are shown in red.

Table 3. Performance metrics of the framework on WSED.

	SLIC [26]	SNIC [27]	ERS [22]	LSC [32]	FH [19]	Ours
F-measure	0.820	0.810	0.814	0.816	0.746	0.822
Precision	0.877	0.867	0.838	0.841	0.834	0.871
Recall	0.796	0.795	0.829	0.829	0.745	0.801

6. Conclusions

In this paper, we present a content-sensitive superpixel generation method with boundary adjustment, which generates compact superpixels that are adapted to image content. Owing to the uneven distribution of seeds, compared to other seed-based methods, the proposed algorithm is more sensitive to the content of the image. The approach tends to generate relatively small and irregular superpixels in complex regions for better boundary adherence, and generates relatively large regular superpixels in flat regions to improve computational efficiency. Taking advantage of boundary adjustment, the proposed algorithm provides results can adapt well to structure changes in natural images. We compared the proposed algorithm with five representative methods on the BSDS 500 dataset. The experimental results demonstrate that superpixels generated by the proposed method outperform the five superpixel algorithms in terms of USE, BR, and ASA. In the future, we will further research the algorithm in a noisy environment. In addition, we plan to apply this approach to applications that require content-sensitive superpixel algorithms.

Author Contributions: Conceptualization, D.Z. and W.B.; Formal analysis, J.R.; Methodology, D.Z., W.B. and X.X.; Software, D.Z. and Z.Z.; Supervision, G.X. and X.X.; Writing—review & editing, G.X. and J.R. All authors have read and agreed to the published version of the manuscript.

Funding: This work was supported in part by Shanxi International Cooperation Project (No. 201803D421039), Key Research and Development Plan of Shanxi Province (No. 201703D111027, No. 201703D111023), the Natural Science Foundation of Shanxi Province (No. 201801D121144, No. 201801D221190), and the Hundreds Talent Program of Shanxi Province, China. This work was also partially supported by the Shaanxi Natural Science Basic Research Project under Grant 2017JQ6058 and the Scientific Research Program funded by Shaanxi Provincial Education Department, China, under Grant 19JK0364.

Conflicts of Interest: The authors declare no conflict of interest.

References

1. Ren, X.; Malik, J. Learning a classification model for segmentation. In Proceedings of the Ninth IEEE International Conference on Computer Vision, Nice, France, 13–16 October 2003; Volume 1, pp. 10–17.
2. Ning, J.; Zhang, L.; Zhang, D.; Wu, C. Interactive image segmentation by maximal similarity based region merging. *Pattern Recognit.* **2010**, *43*, 445–456. [CrossRef]
3. Li, Z.; Wu, X.-M.; Chang, S.-F. Segmentation using superpixels: A bipartite graph partitioning approach. In Proceedings of the 2012 IEEE Conference on Computer Vision and Pattern Recognition IEEE, Providence, RI, USA, 16–21 June 2012; pp. 789–796.
4. Shen, J.; Peng, J.; Dong, X.; Shao, L.; Porikli, F. Higher-Order Energies for Image Segmentation. *IEEE Trans. Image Proc.* **2017**, *26*, 4911–4922. [CrossRef] [PubMed]
5. Dong, X.; Shen, J.; Shao, L.; Gool, L.V. SubMarkov Random Walk for Image Segmentation. *IEEE Trans. Image Proc.* **2016**, *25*, 516–527. [CrossRef] [PubMed]
6. Levinshtein, A.; Sminchisescu, C.; Dickinson, S. Optimal Image and Video Closure by Superpixel Grouping. *Int. J. Comput. Vis.* **2012**, *100*, 99–119. [CrossRef]
7. Perazzi, F.; Krahenbuhl, P.; Pritch, Y.; Hornung, A. Saliency Filters: Contrast Based Filtering for Salient Region Detection. In Proceedings of the 2012 IEEE Conference on Computer Vision and Pattern Recognition, Providence, RI, USA, 16–21 June 2012.
8. Wang, W.; Shen, J.; Shao, L. Video Salient Object Detection via Fully Convolutional Networks. *IEEE Trans. Image Proc.* **2018**, *27*, 38–49. [CrossRef] [PubMed]

9. Wang, W.; Shen, J.; Shao, L. Consistent Video Saliency Using Local Gradient Flow Optimization and Global Refinement. *IEEE Trans. Image Proc.* **2015**, *24*, 4185–4196.
10. Cour, T.; Shi, J. Recognizing objects by piecing together the segmentation puzzle. In Proceedings of the 2007 IEEE Conference on Computer Vision and Pattern Recognition IEEE, Minneapolis, MN, USA, 17–22 June 2007; pp. 1–8.
11. Mori, G.; Ren, X.; Efros, A.A.; Malik, J. Recovering Human Body Configurations: Combining Segmentation and Recognition. In Proceedings of the 2004 IEEE Conference on Computer Vision and Pattern Recognition, Washington, DC, USA, 27 June–2 July 2004; pp. 326–333.
12. He, X.; Zemel, R.S.; Ray, D. Learning and Incorporating Top-Down Cues in Image Segmentation. In Proceedings of the 2006 European Conference on Computer Vision, Graz, Austria, 7–13 May 2006; Volume 3951, pp. 338–351.
13. Nwogu, I.; Corso, J.J. (BP)2: Beyond pairwise Belief Propagation labeling by approximating Kikuchi free energies. In Proceedings of the 2008 IEEE Conference on Computer Vision and Pattern Recognition, Anchorage, AK, USA, 24–26 June 2008; pp. 1–8.
14. Hoiem, D.; Efros, A.A.; Hebert, M. Automatic photo pop-up. *ACM Trans. Gr.* **2005**, *24*, 577–584.
15. Alexe, B.; Deselaers, T.; Ferrari, V. Measuring the Objectness of Image Windows. *IEEE Trans. Pattern Anal Mach. Intell.* **2012**, *34*, 2189–2202. [CrossRef] [PubMed]
16. Bodis-Szomoru, A.; Riemenschneider, H.; Gool, L.V. Superpixel meshes for fast edge-preserving surface reconstruction. In Proceedings of the 2015 IEEE Conference on Computer Vision and Pattern Recognition, Boston, MA, USA, 7–12 June 2015; pp. 2011–2020.
17. Lim, J.; Han, B. Generalized background subtraction using superpixels with label integrated motion estimation. In Proceedings of the 2014 European Conference on Computer Vision, Zurich, Switzerland, 6–12 September 2014; pp. 173–187.
18. Shi, J.; Malik, J. Normalized cuts and image segmentation. *IEEE Trans. Pattern Anal. Mach. Intell.* **2000**, *22*, 888–905.
19. Felzenszwalb, P.F.; Huttenlocher, D.P. Efficient graph-based image segmentation. *Int. J. Comput. Vis.* **2004**, *59*, 167–181. [CrossRef]
20. Moore, A.P.; Prince, S.J.; Warrell, J.; Mohammed, U.; Jones, G. Superpixel lattices. In Proceedings of the 2008 IEEE Conference on Computer Vision and Pattern Recognition IEEE, Anchorage, AK, USA, 23–28 June 2008; pp. 1–8.
21. Veksler, O.; Boykov, Y.; Mehrani, P. Superpixels and Supervoxels in an Energy Optimization framework. In Proceedings of the European Conference on Computer Vision, Crete, Greece, 5–11 September 2010; pp. 211–224.
22. Liu, M.-Y.; Tuzel, O.; Ramalingam, S.; Chellappa, R. Entropy rate superpixel segmentation. In Proceedings of the 2011 IEEE Conference on Computer Vision and Pattern Recognition IEEE, Providence, RI, USA, 20–25 June 2011; pp. 2097–2104.
23. Van den Bergh, M.; Boix, X.; Roig, G.; Van Gool, L. Seeds: Superpixels extracted via energy-driven sampling. *Int. J. Comput.Vis.* **2015**, *111*, 298–314. [CrossRef]
24. Levinshtein, A.; Stere, A.; Kutulakos, K.N.; Fleet, D.J.; Dickinson, S.J.; Siddiqi, K. Turbopixels: Fast superpixels using geometric flows. *IEEE Trans. Pattern Anal. Mach. Intell.* **2009**, *31*, 2290–2297. [CrossRef] [PubMed]
25. Wang, P.; Zeng, G.; Gan, R.; Wang, J.; Zha, H. Structure-Sensitive Superpixels via Geodesic Distance. *Int. J. Comput. Vis.* **2013**, *103*, 1–21. [CrossRef]
26. Achanta, R.; Shaji, A.; Smith, K.; Lucchi, A.; Fua, P.; Süsstrunk, S. SLIC superpixels compared to state-of-the-art superpixel methods. *IEEE Trans. Pattern Anal. Mach. Intell.* **2012**, *34*, 2274–2282. [CrossRef] [PubMed]
27. Achanta, R.; Susstrunk, S. Superpixels and polygons using simple non-iterative clustering. In Proceedings of the 2017 IEEE Conference on Computer Vision and Pattern Recognition, Honolulu, HI, USA, 21–26 July 2017; pp. 4651–4660.
28. Liu, Y.-J.; Yu, C.-C.; Yu, M.-J.; He, Y. Manifold SLIC: A fast method to compute content-sensitive superpixels. In Proceedings of the 2016 IEEE Conference on Computer Vision and Pattern Recognition, Las Vegas, NV, USA, 26 June–1 July 2016; pp. 651–659.
29. Liu, Y.-J.; Yu, M.; Li, B.-J.; He, Y. Intrinsic manifold SLIC: A simple and efficient method for computing content-sensitive superpixels. *IEEE Trans. Pattern Anal. Mach. Intell.* **2018**, *40*, 653–666. [CrossRef] [PubMed]

30. Shen, J.; Du, Y.; Wang, W.; Li, X. Lazy random walks for superpixel segmentation. *IEEE Trans. Image Proc.* **2014**, *23*, 1451–1462. [CrossRef] [PubMed]
31. Shen, J.; Hao, X.; Liang, Z.; Liu, Y.; Wang, W.; Shao, L. Real-time superpixel segmentation by DBSCAN clustering algorithm. *IEEE Trans. Image Proc.* **2016**, *25*, 5933–5942. [CrossRef] [PubMed]
32. Chen, J.; Li, Z.; Huang, B. Linear Spectral Clustering Superpixel. *IEEE Trans. Image Proc.* **2017**, *26*, 3317–3330. [CrossRef] [PubMed]
33. Martin, D.; Fowlkes, C.; Tal, D.; Malik, J. A database of human segmented natural images and its application to evaluating segmentation algorithms and measuring ecological statistics. In Proceedings of the Eighth IEEE International Conference on Computer Vision IEEE, Vancouver, BC, Canada, 7–14 July 2001; Volume 2, pp. 416–423.
34. Prim, R.C. Shortest connection networks and some generalizations. *Bell Syst. Tech. J.* **1957**, *36*, 1389–1401. [CrossRef]
35. Alpert, S.; Galun, M.; Brandt, A.; Basri, R.A. Image Segmentation by Probabilistic Bottom-Up Aggregation and Cue Integration. In Proceedings of the IEEE Conference on Computer Vision and Pattern Recognition, Minneapolis, MN, USA, 17–22 June 2007.